Hindawi
Cellular Microbiology
Volume 2023, Article ID 4091825, 18 pages
https://doi.org/10.1155/2023/4091825

Research Article

Akkermansia muciniphila Ameliorates Lung Injury in Smoke-Induced COPD Mice by IL-17 and Autophagy

Li Zhang, Junjuan Lu, and Caihong Liu

Department of Pulmonary and Critical Care Medicine, The Third Xiangya Hospital of Central South University, Changsha, Hunan 410013, China

Correspondence should be addressed to Caihong Liu; 15874188270@126.com

Received 29 October 2022; Revised 15 February 2023; Accepted 1 March 2023; Published 15 March 2023

Academic Editor: Jayaprakash Narayana Kolla

Objective. Smoking is a primary hazard factor for chronic obstructive pulmonary disease (COPD), which induced a decrease in intestinal *Akkermansia muciniphila* abundance and Th17 imbalance in COPD. This study analyzed the changes of gut microbiota metabolism and *Akkermansia* abundance in patients with smoking-related COPD and explored the potential function of *Akkermansia muciniphila* in smoke-induced COPD mice. *Methods*. Gut microbiota diversity and metabolic profile were analyzed by 16S rRNA sequence and metabolomics in COPD patients. The IL-1β, IL-17, TNF-α, and IL-6 levels were tested by ELISA. Lung tissue damage was observed by HE staining. The expression of cleave-caspase 3, trophoblast antigen 2 (TROP2), and LC3 in lung tissues were analyzed by IHC or IF. The p-mTOR, mTOR, p62, and LC3 expression in lung tissues were tested by western blot. *Results*. The levels of IL-17, IL-1β, TNF-α, and IL-6 in the peripheral blood of COPD patients increased significantly. The number and alpha diversity of gut microbiota were decreased in COPD patients. The abundance of *Akkermansia muciniphila* in gut of COPD patients was decreased, and the metabolic phenotype and retinol metabolism were changed. In the retinol metabolism, the retinol and retinal were significantly changed. *Akkermansia muciniphila* could improve the alveolar structure and inflammatory cell infiltration in lung tissue, reduce the IL-17, TNF-α, and IL-6 levels in peripheral blood, promote the p-mTOR expression, and inhibit the expression of autophagy-related proteins in smoke-induced COPD mice. *Conclusion*. The number and alpha diversity of gut microbiota were decreased in patients with smoking-related COPD, accompanied by decreased abundance of *Akkermansia muciniphila*, and altered retinol metabolism function. Gut *Akkermansia muciniphila* ameliorated lung injury in smoke-induced COPD mice by inflammation and autophagy.

1. Introduction

Chronic obstructive pulmonary disease (COPD) is a significant cause of morbidity and the third leading cause of death worldwide [1]. Its incidence increases yearly as the population ages and personal and socioeconomic costs increase [2]. Despite decades of research, and the growing healthcare and societal burden of COPD, therapeutic COPD breakthroughs have not occurred [3]. Healthy respiratory microbiota was in a dynamic balance of migration and removal, and the levels of some specific groups in the lung microbiome change over the course of COPD [4]. Metagenomic data analysis showed that butyrate, homocysteine, and palmitate were the biota metabolites with the strongest interactions with host genes associated with COPD [5]. Therefore, exploring the metabolic changes of the microbiota in COPD patients may be helpful for the development of new therapeutic methods.

Clinical studies have shown that the stability of lung microbiota decreases with the time of deterioration, and that bacteria such as *Haemophilus* and *Moraxella* are associated with disease severity, worsening events, and bronchiectasis [6]. The diversity of microbiota in COPD patients was lower than that in healthy [7]. Oral administration of an isolated strain of *Parabacteroides* Gorei (Pg, MTS01) alleviated COPD by reducing intestinal inflammation, enhancing the activity of mitochondria and ribosomes in colonic cells, restoring abnormal amino acid metabolism, inhibiting lung inflammation, and antagonizing TLR4 signaling pathway [8]. These studies prove that the communication between

gut microbiota may contribute to the prevention or treatment of COPD.

PM2.5 was a primary air pollutant that could cause airway injury, which could inhibit autophagy and promote lung inflammation and fibrosis by inducing IL-17A secretion and mediating PI3K/Akt/mTOR signaling pathway [9]. In addition, IL-17 induced autophagy and promoted fibrosis and mitochondrial dysfunction in bronchial fibroblasts [10]. MAP1-LC3B mice developed IL-17A-dependent pathology in lung after respiratory syncytial virus (RSV) infection, suggesting that ER stress-dependent and autophagy cytokines initiated and maintained the aberrant Th17 response [11]. These studies demonstrated that IL-17-mediated autophagy occurred in the pathological of COPD, but the specific mechanism remains unknown.

Intestinal microbiome aberrations are increasingly implicated in the pathogenesis of several infectious and non-infectious diseases [12]. Autophagy is the key for the immune system to eliminate pathogenic bacteria, control inflammation, and immune-microbiome balance [13]. The abundance of *Akkermansia muciniphila* was reduced in asthmatic patients, which may inhibit inflammation by secreting or synthesizing metabolites [14]. However, the Bacteroidetes and Proteobacteria were increased, while *Akkermansia muciniphila* was decreased in IL-17Ra$^{-/-}$ mice with HFD [15]. In addition, *Akkermansia muciniphila* colonization and increased symbiosis in early life contribute to the maintenance of host intestinal barrier by stachyose increasing SCFA levels and decreasing LPS, IL-1, IL-17, and TNF-α levels [16]. Accordingly, we hypothesized that the abundance of *Akkermansia muciniphila* might be related to IL-17 immunity. Patients with COPD have evidence of systemic inflammation, which is associated with impaired lung function, especially in those who smoke heavily [17, 18]. In addition, persistence of systemic inflammation in patients with COPD is associated with poor clinical outcomes (all-cause mortality and frequency of exacerbations) [19]. Cigarette smoke [20] and cigarette smoke extract were known to induce decreased intestinal *Akkermansia* abundance, Th17/Treg imbalance, and inflammatory cell infiltration and decreased lung function in COPD mice [21]. Therefore, this study analyzed the phenotypic changes of intestinal microbiota metabolism in clinical COPD patients. The cigarette-induced COPD mouse model was constructed to explore the interaction between intestinal microbial metabolism, *Akkermansia muciniphila* abundance changes, peripheral blood IL-17 secretion, and autophagy in COPD to provide a new therapy for COPD.

2. Material and Methods

2.1. Source of Clinical Patients and Diagnostic Criteria. Both the COPD patients ($n = 11$) and the male patients without COPD ($n = 11$) were from the Department of Pulmonary and Critical Care Medicine, the Third Xiangya Hospital of Central South University. According to the diagnostic criteria [7], clinical epidemiologists conducted multistage-stratified sampling for COPD and non-COPD samples. They established COPD group and non-COPD group with matched age, sex, BMI, smoking, or not. The inclusion criteria of COPD patients were as follows: (1) consistent with persistent respiratory symptoms and irreversible airflow limitation, FEVI/FVC < 0.70 after bronchodilator inhalation; (2) 40-80 years old; and (3) stable chest CT and pulmonary function examination were performed in the past 12 months. COPD exclusion criteria were as follows: bronchial asthma, interstitial lung disease, pneumoconiosis, silicosis, pulmonary infection, and pulmonary nodules > 3 cm. In addition, the inclusion criteria of non-COPD patients were as follows: (1) 40-80 years old; (2) with pulmonary function test records and normal; and (3) chest CT data were recorded. Non-COPD exclusion criteria were history or diagnosis of bronchial asthma, pneumoconiosis, silicosis, diffuse pulmonary interstitial fibrosis, etc. Both fecal and blood samples were collected from the same patients for subsequent analysis. All patients signed informed consent. The study was approved by the Ethics Committee of the Third Xiangya Hospital of Central South University (no. 2022-S133). All processes were implemented in accordance with the Declaration of Helsinki (1964).

2.2. Construction and Grouping of COPD Mouse Model. The commercial unfiltered cigarettes (cigarettes from Hunan Tobacco Industry Co., LTD., Changsha, China) containing tar (11 mg) and nicotine (0.9 mg) per cigarette were applied. Twenty-four 8-week-old male C57BL/6J mice (Hunan Slyke Jingda Laboratory Animal Co., Ltd., Changsha, China) were set to the following three groups: the control group, the COPD group (cigarette smoke+LPS modeling) [21], and the *Akkermansia muciniphila* group (on the basis of COPD group, oral gavage of *Akkermansia muciniphila*). In brief, mice were raised in perspex chambers with disposable filters. During the 1st week, the animals were exposed to 4 cigarettes/d for 5 d/w. The mice were then exposed to smoke from six cigarettes a day until week 6. At the end of 3 w and 5 w, mice were injected intratracheal with LPS (750 ng/kg, Sigma-Aldrich, St. Louis, USA). After the last cigarette smoke exposure for 1 w, mice were euthanized. The blood, bronchoalveolar lavage fluid (BALF), and lung tissue were collected. The study was approved by the Ethics Committee of Xiangya Third Hospital of Central South University (no. 2022-S133).

2.3. Enzyme-Linked Immunosorbent Assay (ELISA). The blood samples were placed and centrifuged at 1000 g for 15 min at 2-8°C to collect supernatant. The TNF-α (mouse, KE10002, Proteintech, Chicago, USA), IL-17 (mouse, KE10020, Proteintech, Chicago, USA), IL-6 (mouse, KE10007, Proteintech, Chicago, USA), TNF-α (human, KE00154, Proteintech, Chicago, USA), IL-17A (human, KE00203, Proteintech, Chicago, USA), IL-6 (human, KE00139, Proteintech, Chicago, USA), and IL-1β (human, KE00021, Proteintech, Chicago, USA) kits were used to analyze the cytokine in serum samples on the microplate analyzer (MB-530, HEALES, Shenzhen, China).

2.4. Hematoxylin-Eosin (HE) Staining. The lung tissue was fixed, sliced, and baked for 12 hours. Sections were dewaxed and stained with hematoxylin (Abiowell, Changsha, China)

Table 1: Baseline information of patients.

Items	Control	COPD	*P* value
Individuals	$n = 11$	$n = 11$	
Age (years)	60.52 ± 7.44	65.90 ± 8.24	0.074
BMI	17.96 ± 2.15	19.23 ± 2.95	0.061
Systolic blood pressure	117.94 ± 19.42	118.81 ± 21.08	0.863
Diastolic blood pressure	58.74 ± 12.66	69 ± 10.93	0.918
Pulse	78.12 ± 14.06	90.18 ± 19.19	0.041
Disease status			
GOLD I	NA	0	
GOLD II	NA	2	
GOLD III	NA	3	
GOLD IV	NA	6	
Lung function			
FVC(L/min)	3.52 ± 0.44	2.09 ± 0.69	0.016
FVC % predict	86.52 ± 16.14	63.52 ± 20.41	<0.01
FEV1(L/min)	1.74 ± 0.22	0.99 ± 0.51	<0.01
FEV1 % predict	87.14 ± 14.63	38.22 ± 20.64	<0.01
FEV/FVC ratio	76.39 ± 8.24	45.69 ± 10.34	<0.01
FEV1/FVC ratio % predicted	84.32 ± 9.15	55.33 ± 11.70	<0.01
Blood count			
Haemoglobin (g/L)	102.06 ± 10.12	113.72 ± 18.94	0.354
WBC ($\times 10^9$/L)	6.14 ± 1.42	7.23 ± 2.56	<0.01
RBC ($\times 10^{12}$/L)	3.72 ± 0.28	3.78 ± 0.40	0.241
MCV (fL)	49.96 ± 17.66	51.43 ± 21.89	0.896
MCH (pg)	27.23 ± 1.85	27.27 ± 2.12	0.984
RDW (%)	32.24 ± 6.14	34.08 ± 8.59	0.752
Platelets ($\times 10^9$/L)	218.32 ± 109.12	234.54 ± 116.33	0.674
Neutrophils ($\times 10^9$/L)	4.09 ± 1.24	5.10 ± 2.44	0.085
Lymphocytes ($\times 10^9$/L)	1.20 ± 0.76	1.22 ± 0.84	0.852
Monocytes ($\times 10^9$/L)	0.44 ± 0.08	0.53 ± 0.12	0.027
Eosinophils ($\times 10^9$/L)	0.21 ± 0.07	0.33 ± 0.16	0.042
Basophils ($\times 10^9$/L)	0.02 ± 0.04	0.04 ± 0.21	0.556

and eosin (Abiowell, Changsha, China), respectively. The sections were dehydrated by gradient alcohol (95~100%) and sealed. Finally, the sections were examined on a microscope (BA210T, Motic, Xiamen, China).

2.5. Immunohistochemistry (IHC). The lung tissue sections were immersed in 0.01 M citrate buffer ($pH = 6.0$) in a continuous boiling water bath for 20 min and cooled to room temperature for antigen repair. The sections were added with 1% periodate and kept at room temperature for 10 min to inactivate the endogenous enzymes. The sections were dropped with appropriately diluted primary anti-caspase 3 (1 : 50, ab184787, Abcam, Cambridge, UK) and anti-TROP2 (1 : 50, ab214488, Abcam, Cambridge, UK) overnight. Sections were incubated at 37°C with CoraLite488-conjugated goat anti-rabbit IgG (H+L, 50-100 μL, SA00013-2, Proteintech, Chicago, USA). DAB working solution (ZSGB-BIO, Beijing, China) was added to the sections for staining. Sections were counterstained with hematoxylin (Abiowell, Changsha, China). Then, the sections were sealed and observed by microscope (BA410T, Motic, Xiamen, China).

2.6. Immunofluorescence (IF). Lung tissue sections were successively incubated in sodium borohydride solution, 75% ethanol solution, and Sudan black dye. Sections were blocked by BSA (5%). Sections were incubated with appropriate dilutions of anti-LC3 (1 : 50, 14600-1-AP, Proteintech, Chicago, USA), and anti-rabbit IgG (H+L, 50-100 μL, SA00013-2, Proteintech Chicago, USA). Sections were stained with DAPI working solution (Abiowell, Changsha, China) at 37°C. The sections were sealed with buffer glycerin

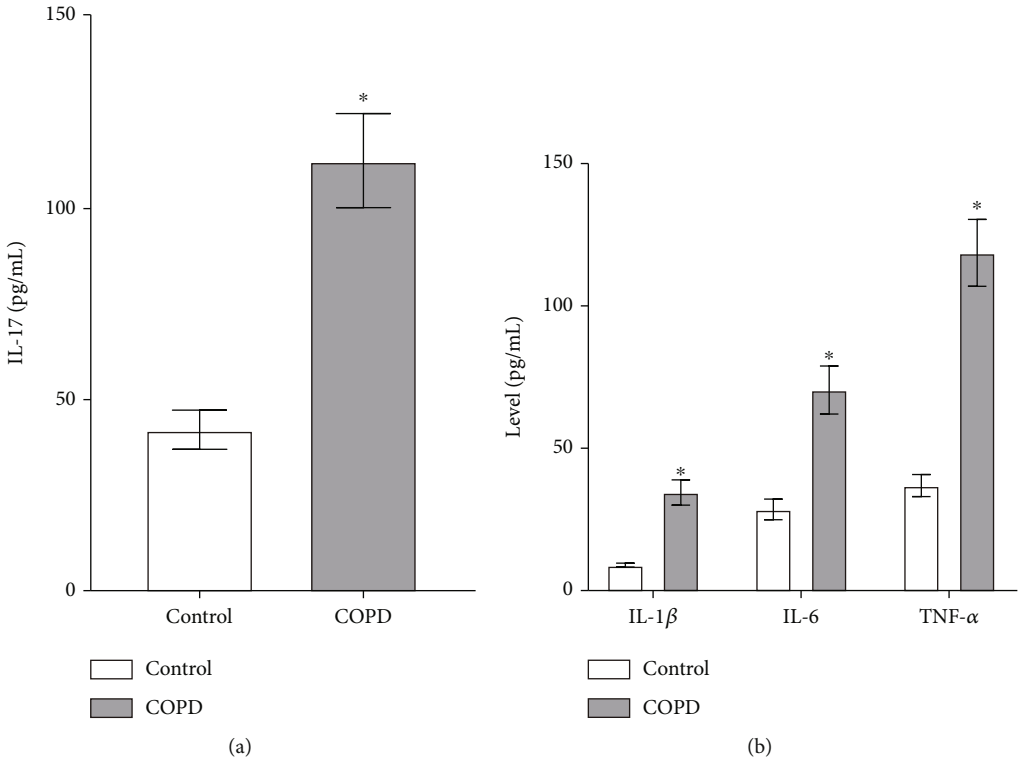

Figure 1: Changes of serum inflammatory in patients. (a) The level of IL-17 was analyzed by ELISA. (b) The levels of IL-1β, IL-6, and TNF-α were analyzed by ELISA. $^*P < 0.05$ vs. control.

(Abiowell, Changsha, China). Then, sections were observed by the microscope (BA410T, Motic, Xiamen, China).

2.7. Western Blot. At the end of the experiment, lung tissues were collected. The extraction and concentration of protein were detected by RIPA (AWB0136, Abiowell, Changsha, China) and BCA, respectively. Proteins were separated by 12% SDS-PAGE. The proteins were transferred to the PVDF membranes blocked with 5% nonfat milk (AWB0004, Abiowell, Changsha, China). The incubated primary antibodies included anti-LC3 (1 : 1000, 14600-1-AP, Proteintech, Chicago, USA), anti-p62 (1 : 1000, 18420-1-AP, Proteintech, Chicago, USA), anti-p-mTOR (1 : 5000, ab109268, Abcam, Cambridge, UK), anti-mTOR (1 : 10000, ab134903, Abcam, Cambridge, UK) and anti-β-actin (1 : 5000, 66009-1-Ig, Proteintech, Chicago, USA). Membranes were incubated with anti-mouse IgG (1 : 500, AWS0001, Abiowell, Changsha, China) and anti-rabbit IgG (1 : 500, AWS0002, Abiowell, Changsha, China) for 90 min at 37°C. Then, SuperECL Plus (AWB0005, Abiowell, Changsha, China) was used for visualization and imaging analysis.

2.8. 16S rRNA Sequencing. The DNA in fecal samples was extracted and detected by DNA extraction kit (CAT.#DP328-02, Tiangen, Beijing, China) and Qubit, respectively. Phusion enzyme (K1031, APExBIO, Houston, USA) and bacterial primers (V3-V4 region) were applied for library construction. Illumina NovaseQ6000 PE250 (Illumina, San Diego, USA) was applied for sequencing to obtain raw data. QIIME2 (2020.2) and DADA2 were applied and invoked for quality control and alpha diversity analysis. Species annotation was made for each ASV sequence by reference to the SilvA-132-99 database. R software (VennDiagram) and jvenn web page were used to visualize common and unique microbiota between groups. Based on PICRUSt (https://github.com/picrust/picrust2) and MetaCyc database (https://metacyc.org/), microbial function was predicted.

2.9. Metabolomics. Liquid chromatography tandem mass spectrometry/mass spectrometry (LC-MS/MS) analyses were performed to obtain MS raw data files. Raw data were converted and processed by R package XCMS (version 3.2). The preprocessing results generated a data matrix that consisted of the retention time (RT), mass-to-charge ratio (m/z) values, and peak intensity. The R package CAMERA was used for peak annotation after XCMS data processing. MetaboAnalyst platform (https://www.metaboanalyst.ca/) was used for bioinformatics analysis. The Kyoto Encyclopedia of Genes and Genomes (KEGG, https://www.kegg.jp/) pathway database was used for metabolite function prediction.

2.10. Data Statistics and Analysis. GraphPad Prism 8.0 (San Diego, USA) statistical software was used for the statistical analysis of the data. The data were expressed by mean ± standard deviation. First, the normality and homogeneity of variance were tested. The test conformed to the normal distribution, and the variance was homogeneous. The unpaired t-test was applied between groups. The comparison between multiple groups uses one-way ANOVA or ANOVA. The

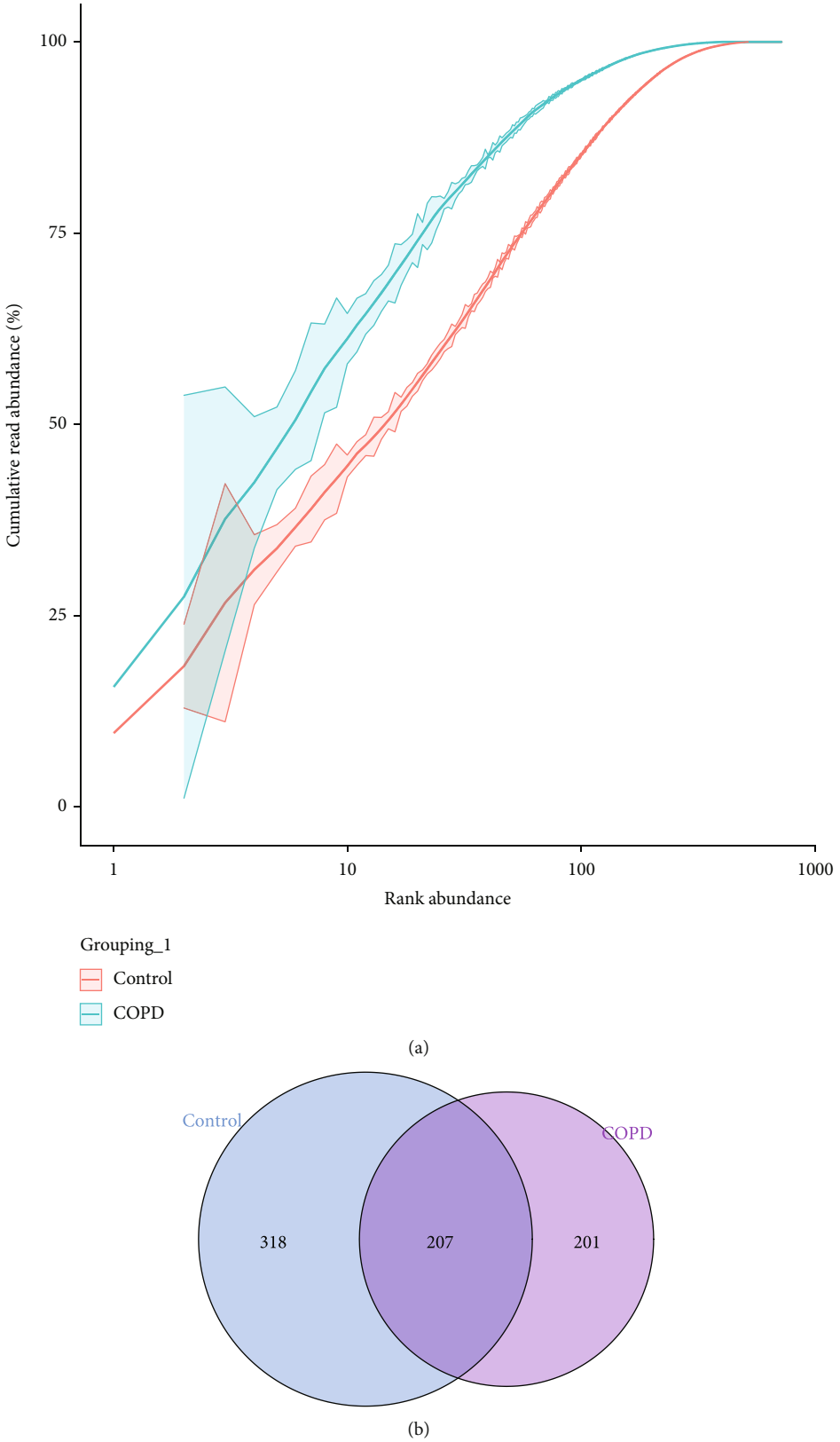

Figure 2: Continued.

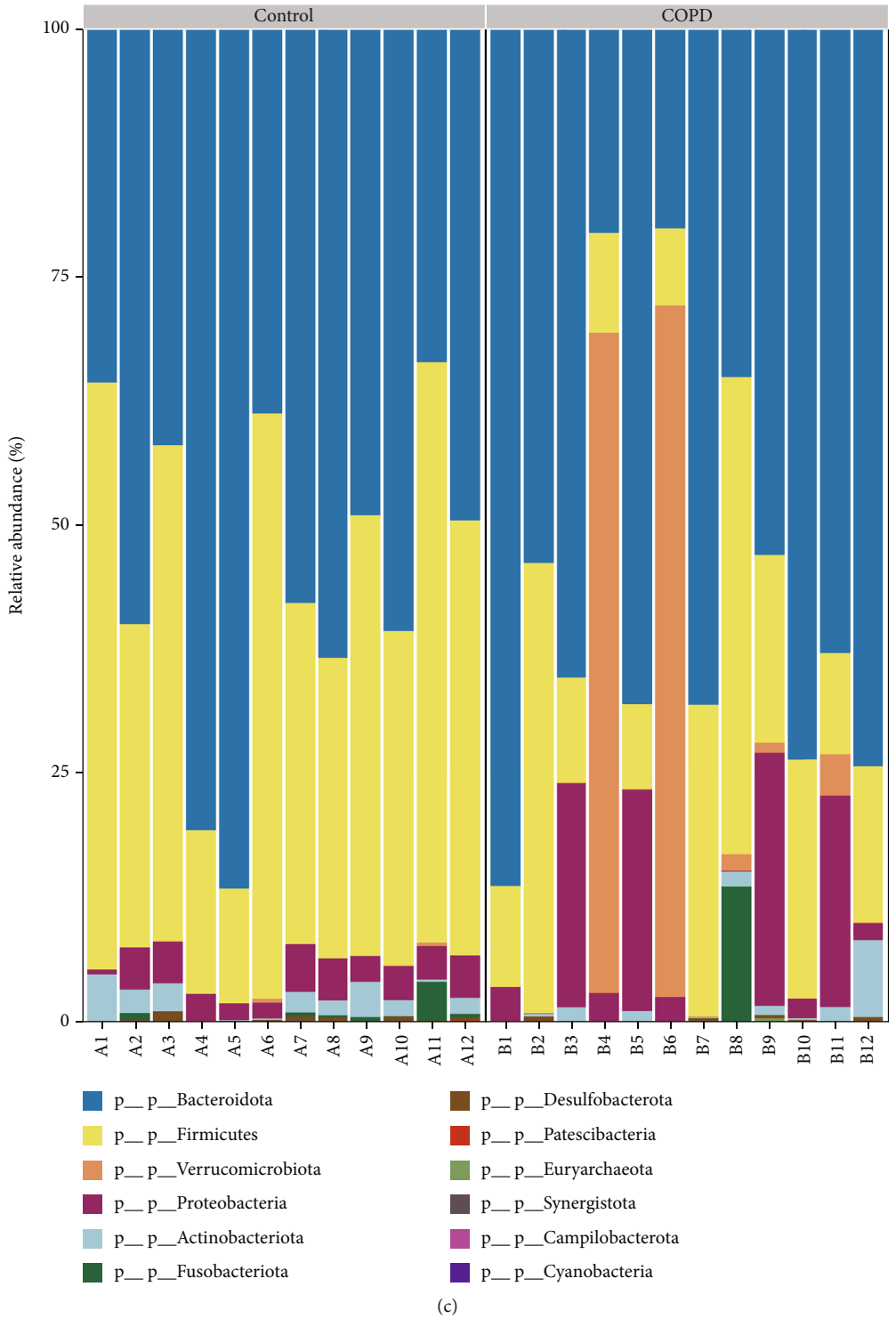

(c)

Figure 2: Continued.

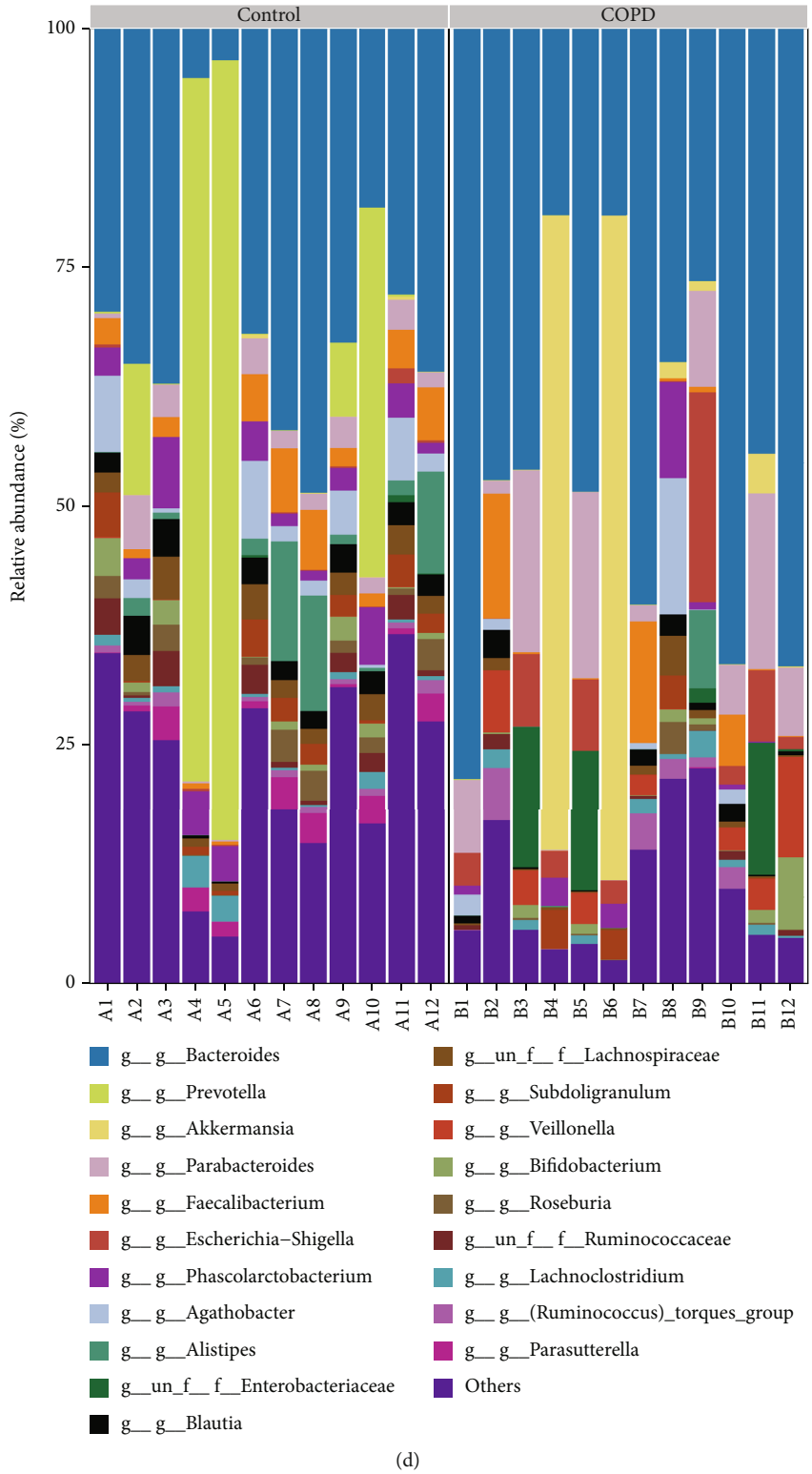

(d)

Figure 2: Analysis of the quantity and abundance of intestinal microbiota in COPD patients and control patients. (a) Rank abundance curve. (b) Venn diagram. (c, d) Relative abundance of species at phylum and genus level.

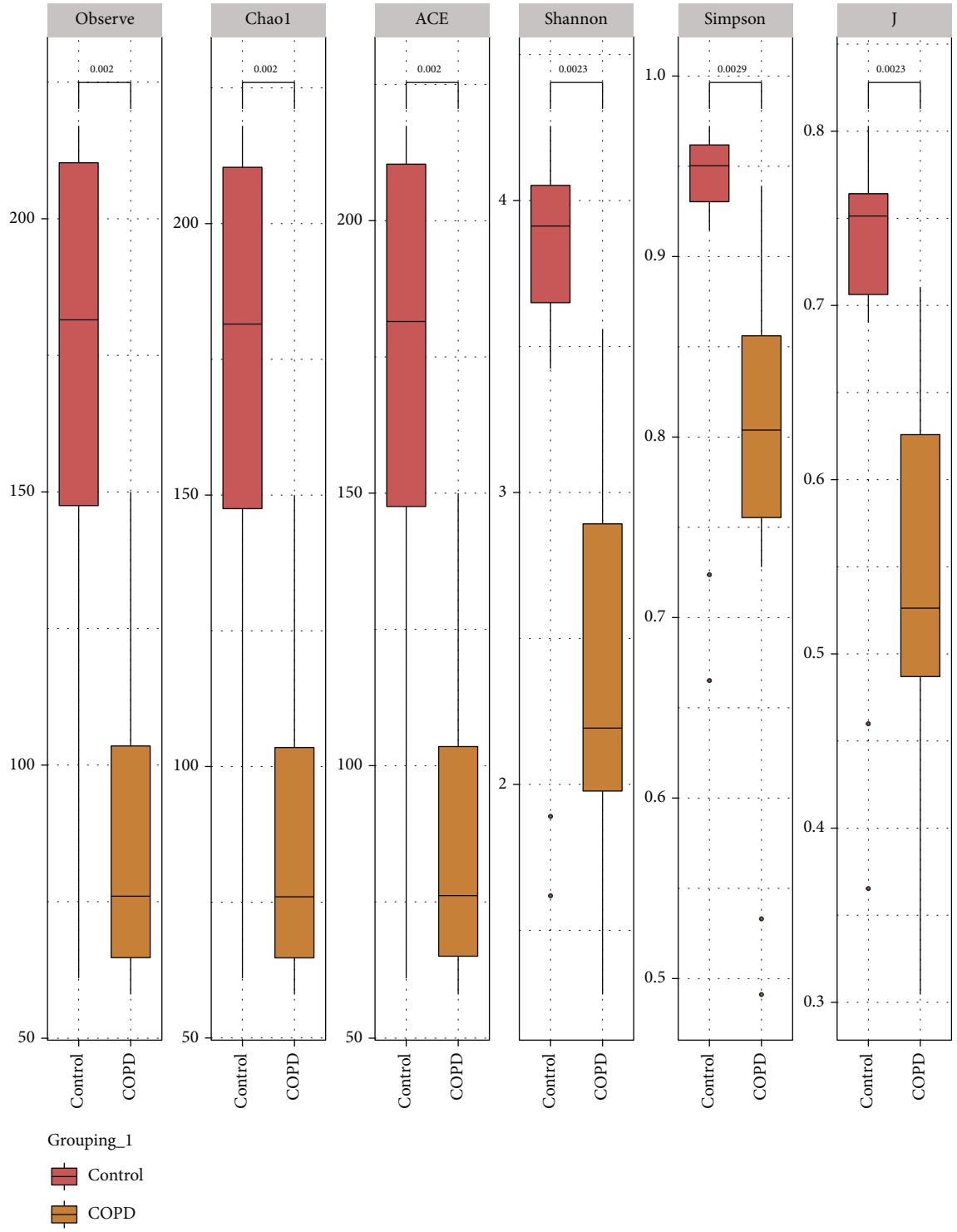

(a)

Figure 3: Continued.

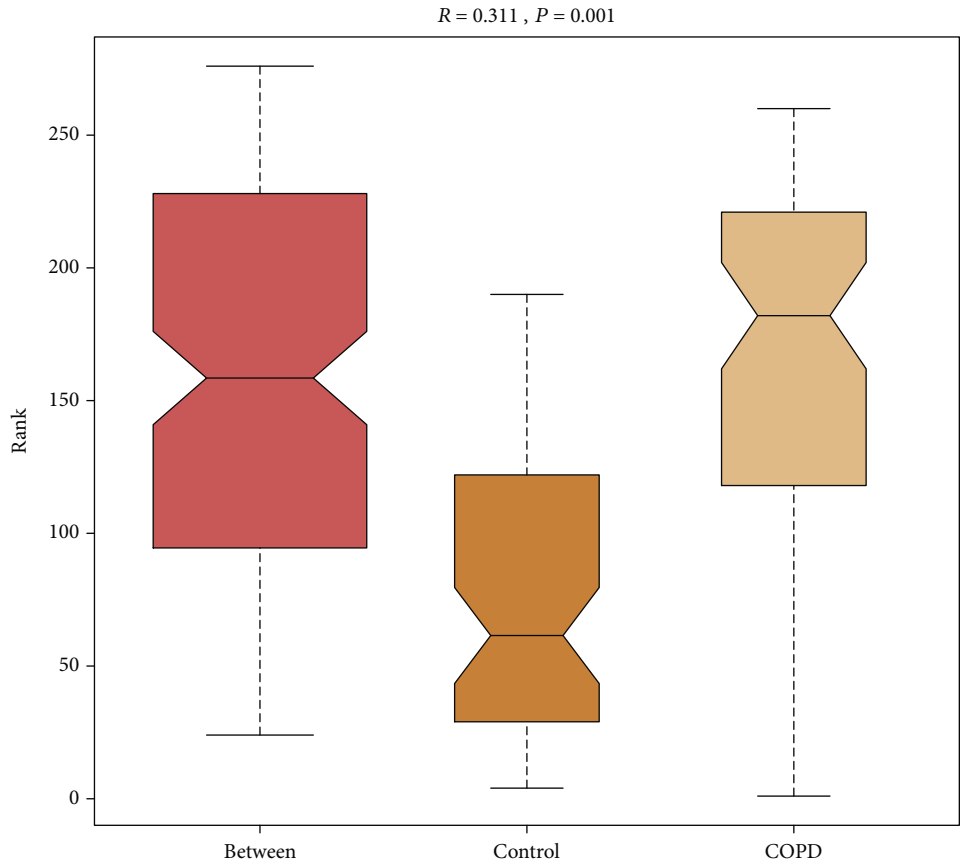

(b)

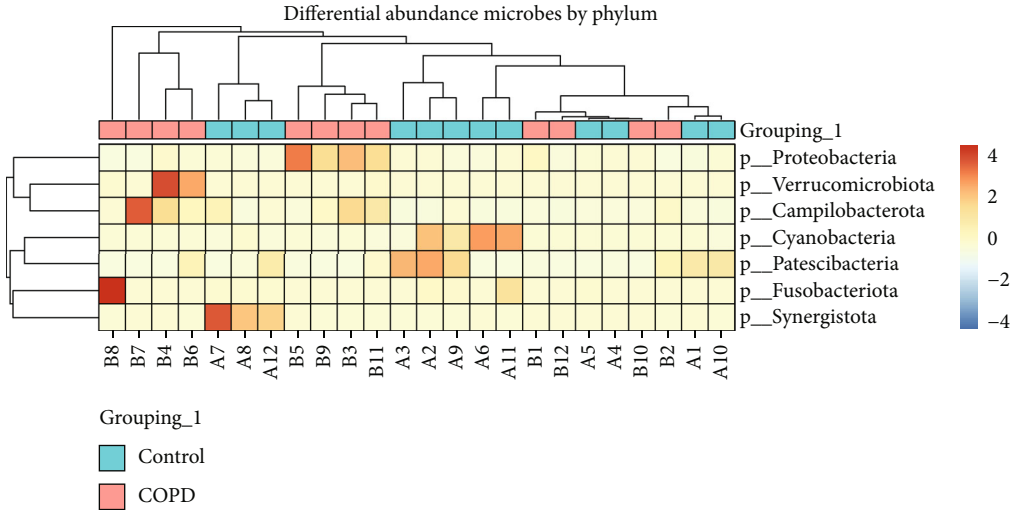

(c)

Figure 3: Continued.

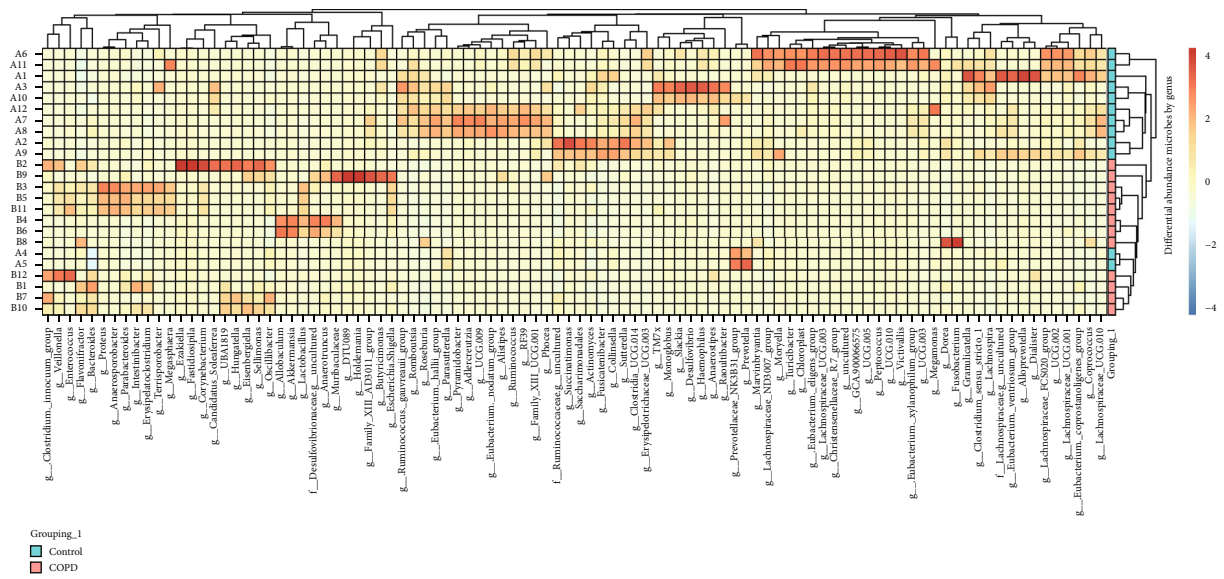

(d)

Figure 3: Diversity and differential changes of intestinal microbiota in COPD patients. (a) Alpha diversity index. (b) Beta diversity index. (c,d) Heatmap of species difference at phylum and genus level.

Tukey post hoc test was used. $P < 0.05$ meant the difference was statistically significant.

3. Results

3.1. Clinical Characteristics and Inflammation Levels in Patients with COPD. Baseline analysis of clinical patients showed that the pulse index was increased significantly and the lung function index was decreased significantly in COPD patients (Table 1). In addition, WBC, monocytes, and eosinophils indices in the blood count of COPD patients were significantly increased (Table 1). The IL-17, IL-1β, IL-6, and TNF-α levels were increased significantly in the peripheral blood of COPD patients (Figures 1(a) and 1(b)). These results proved that COPD patients were associated with decreased lung function and increased peripheral blood inflammation.

3.2. Number and Species Annotation Analysis of Gut Microbiota in COPD. Rank abundance gradually increased with the increase of sequencing depth and reached a plateau, which proved sequence depth was sufficient for subsequent analysis (Figure 2(a)). Venn plot showed the quantity of gut microbes was reduced in COPD patients (Figure 2(b)). Species annotation showed that the Bacteroidota, Firmicutes, Verrucomicrobiota, Proteobacteria, Actinobacteriota, Fusobacteriota, Desulfobacterota, Patescibacteria, Euryarchaeota, Synergistota, Campilobacterota, and Cyanobacteria were markedly enriched at the phylum level (Figure 2(c)). The *Bacteroides*, *Prevotella*, *Akkermansia*, *Parabacteroides*, *Faecalibacterium*, *Escherichia-Shigella*, *Phascolarctobacterium*, *Agathobacter*, *Alistipes*, *Blautia*, *Subdoligranulum*, *Veillonella*, *Bifidobacterium*, *Roseburia*, *Lachnoclostridium*, *[Ruminococcus]_torques_group*, and *Parasutterella* were markedly enriched at the genus level (Figure 2(d)). These results suggest that COPD is followed with a decrease in the quantity of gut microbes, but the specific microbial changes still need to be further analyzed.

3.3. Diversity and Differential Changes of Gut Microbiota in COPD. Alpha diversity index analysis showed that the alpha diversity index was decreased in the COPD patients (Figure 3(a)). There was a significant difference between groups ($p = 0.001$) (Figure 3(b)). The Cyanobacteria, Synergistota, and Patescibacteria abundance were decreased significantly, and the Verrucomicrobiota, Campilobacterota, and Proteobacteria abundance were increased significantly in the intestinal tract of COPD patients (Figure 3(c)). The abundance of *Flavonifractor* and *Muribaculaceae* was significantly decreased; the abundance of *Akkermansia*, *[Eubacterium]_hallii_group*, *[Eubacterium]_ventriosum_group*, *Alistipes*, *Anaerostipes*, *Blautia*, *Collinsella*, *Coprococcus*, *Dorea*, *Erysipelotrichaceae_UCG-003*, *Fusicatenibacter*, *Fusobacterium*, *Lachnospira*, *Lachnospiraceae_UCG-010*, *Monoglobus*, *Parasutterella*, *Phascolarctobacterium*, *Prevotella*, *Romboutsia*, *Roseburia*, and *UCG-002* were increased significantly in the intestinal tract of COPD patients (Figure 3(d)). These results demonstrated that the microbiota diversity of COPD patients decreased, accompanied by a significant change in microbiota level.

3.4. The Changes of Gut Microbiota Function in COPD Patients. We further analyzed the abundance changes of *Akkermansia* species, and the results showed that the *g_Akkermansia. S_Akkermansia muciniphila* abundance was significantly decreased, while the abundance of *g_Akkermansia. S_uncultured bacterium* was increased significantly in the intestine of COPD patients (Figure 4(a)). MetaCyc data annotation and functional analysis revealed that protocatechuate degradation I (meta-cleavage pathway), superpathway of

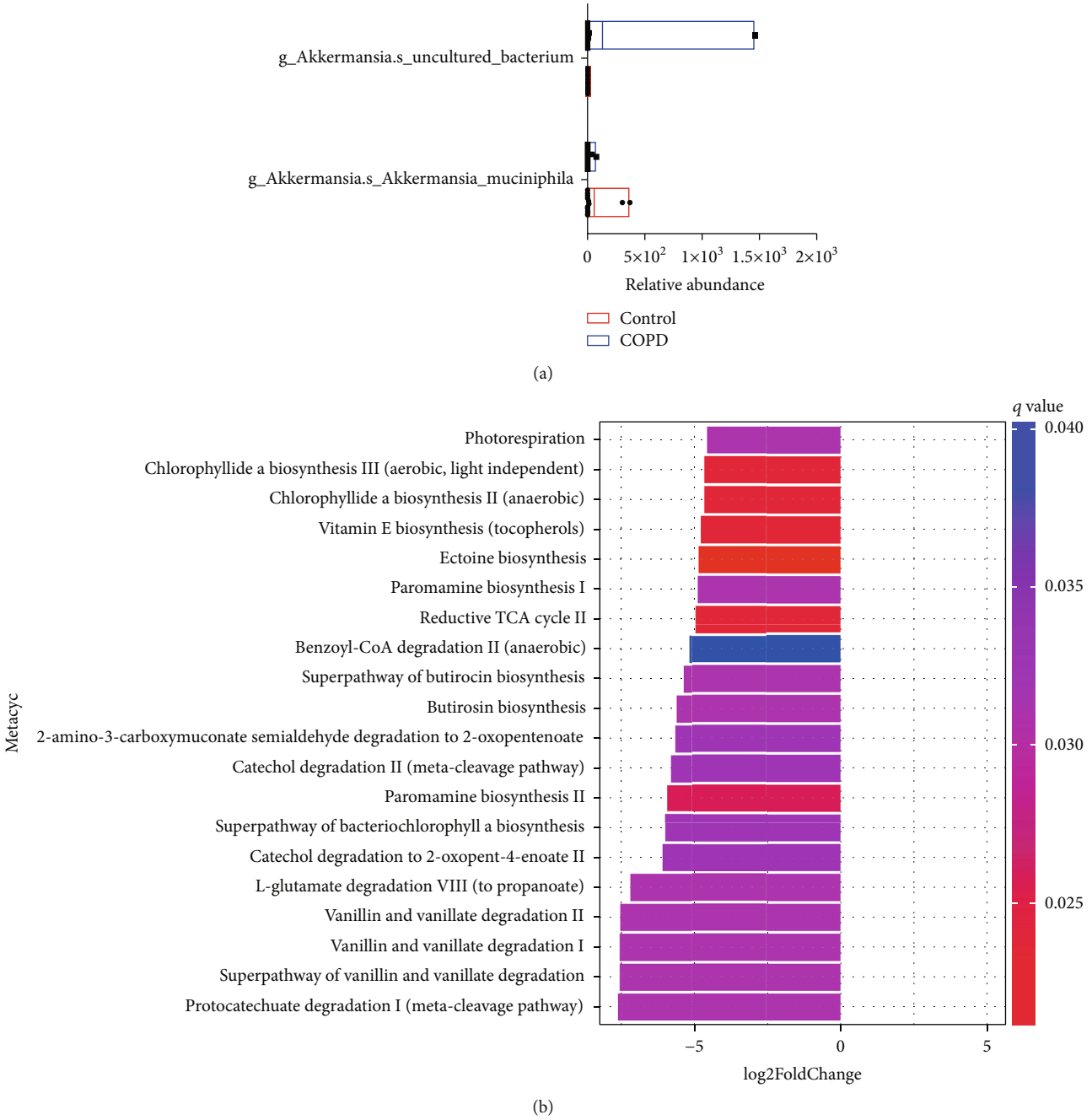

Figure 4: Species abundance of *Akkermansia* and functional annotation of gut microbiota at MetcyC. (a) The species abundance of the genus *Akkermansia* at the species level. (b) Metcyc annotated the functional changes of gut microbiota.

vanillin and vanillate degradation, vanillin and vanillate degradation I, vanillin and vanillate degradation II, L-glutamate degradation VIII (to propanoate), catechol degradation to 2-oxopent-4-enoate II, superpathway of bacteriochlorophyll a biosynthesis, and vitamin E biosynthesis (tocopherols) pathways are significantly depleted in the gut of patients with COPD (Figure 4(b)). Therefore, *Akkermansia muciniphila* may be a potential probiotic for improving microbial structure and function in the treatment of gut microbiota diversity in COPD patients.

3.5. Changes of Gut Metabolic Phenotype in COPD Patients. PLSDA analysis showed significant differences between groups (Figure 5(a)). Fold change plots showed that the abundance of 123 metabolites changed between groups (Figure 5(b)). The volcano map showed significant changes in the abundance of 47 metabolites (Figure 5(c)). Pentadecanoic acid, 4-acetamidobutyric acid, octylamine, xanthurenate, 4-imidazoleacetate, uvaol, indolelactic acid, and guanosine were significantly increased in COPD (Figure 5(c)). 7-Ketocholesterol, uridine diphosphate glucose, uridine diphosphate

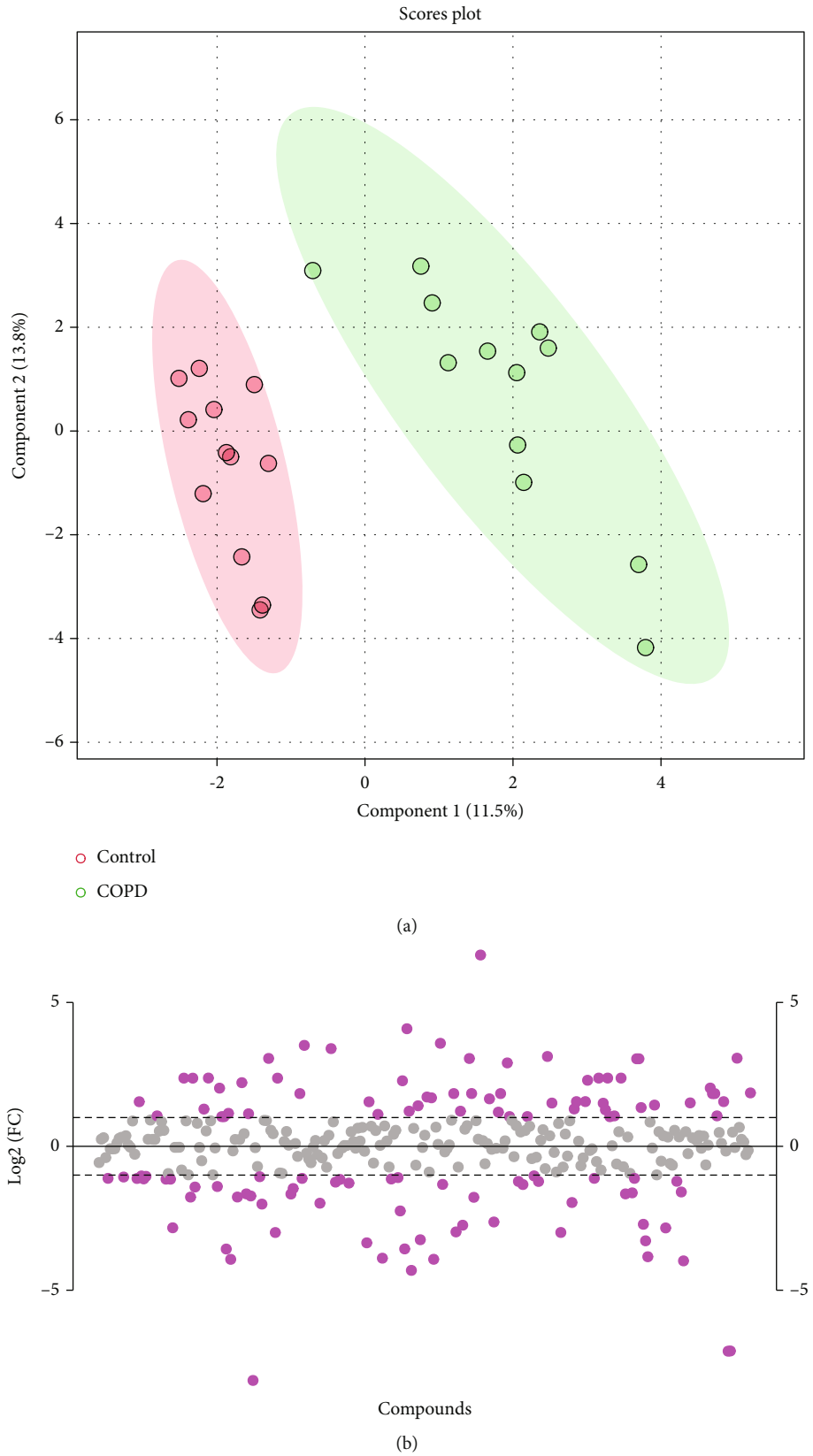

Figure 5: Continued.

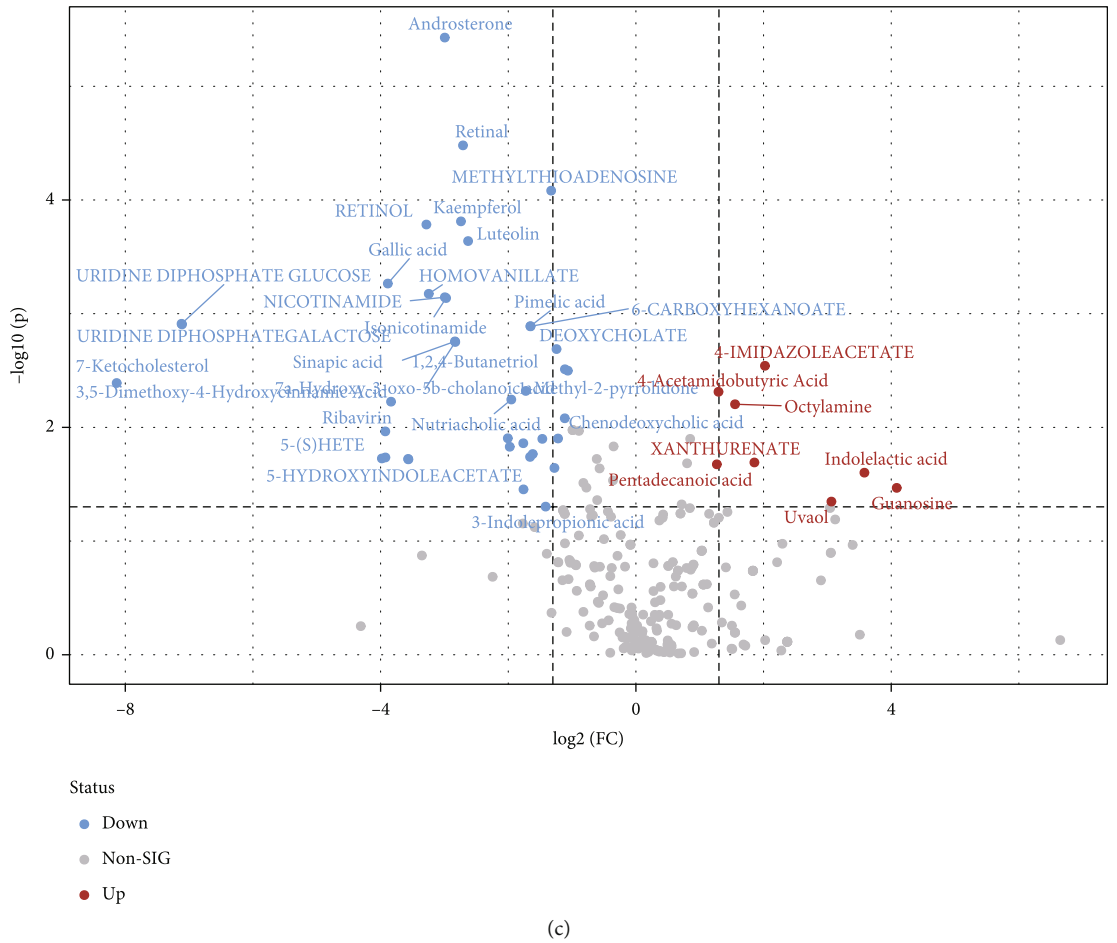

(c)

Figure 5: Metabolomics reveals the changes of intestinal metabolic phenotype in COPD patients. (a) PLSDA analysis. (b) Fold change. (c) Volcano plot.

galactose, taurodeoxycholic acid, 5-(S)HETE, indoleacetaldehyde, gallic acid, ribavirin, 4-methylcatechol, guaiacol, retinol, homovanillate, androsterone, nicotinamide, isonicotinamide, sinapic acid, 3,5-dimethoxy-4-hydroxycinnamic acid, kaempferol, retinal, luteolin, adenosine monophosphate, creosol, nutriacholic acid, 3-hydroxybenzyl alcohol, 5-hydroxyindoleacetate, 7a-hydroxy-3-oxo-5b-cholanoic acid, biliverdin, pimelic acid, 6-carboxyhexanoate, pregnenolone sulfate, biocytin, 3-indolepropionic acid, methylthioadenosine, dodecanedioic acid, deoxycholate, n-acetylalanine, chenodeoxycholic acid, 1,2,4-butanetriol, and 1-methyl-2-pyrrolidone were significantly decreased in COPD (Figure 5(c)). KEGG prediction analysis showed that the retinol metabolism was significantly changed in COPD intestine, in which the metabolites of retinol and retinal were significantly changed, which may be related to the metabolism status of the patients (Supplementary Figure 1). These results suggested that the intestinal metabolic phenotype and function of COPD patients were altered.

3.6. Akkermansia Muciniphila Improved Lung Tissue Injury and Autophagy in COPD Mice. The alveolar structure was clear, the alveolar wall was intact and continuous, and a small number of inflammatory cells could be seen in the alveolar septum in the control group (Figure 6(a)). The alveolar structure of COPD mice was destroyed, most of the alveoli fused with each other to form a large alveolar cavity, and there was obvious inflammatory cell infiltration in the alveolar septum (Figure 6(a)). *Akkermansia muciniphila* intervention significantly improved alveolar structure and inflammatory infiltration in COPD mice (Figure 6(a)). The IL-17, IL-6, and TNF-α levels in the blood of COPD mice were increased (Figure 6(b)). *Akkermansia muciniphila* intervention reduced the levels of IL-17, IL-6, and TNF-α in the blood of COPD mice (Figure 6(b)). TROP2 may affect airway remodeling in COPD smoking patients by increasing basal cell (BC) hyperplasia, EMT-like changes, and introducing inflammatory molecules into the microenvironment to interfere with BC function [22]. The function of caspase-3 may contribute to the persistence of neutrophils (inflammation) in smokers' lungs and is a factor in the higher incidence of community-acquired pneumonia [23]. The cleave-caspase 3, TROP2, and LC3 expression in lung tissue of COPD mice were increased, which was reversed by *Akkermansia muciniphila* (Figures 6(c) and 6(d)). In addition, *Akkermansia muciniphila* promoted the p62 and p-mTOR expressions and inhibited the LC3 protein expression in lung tissues of COPD mice (Figures 6(e) and 6(f)). These results demonstrated that *Akkermansia muciniphila*

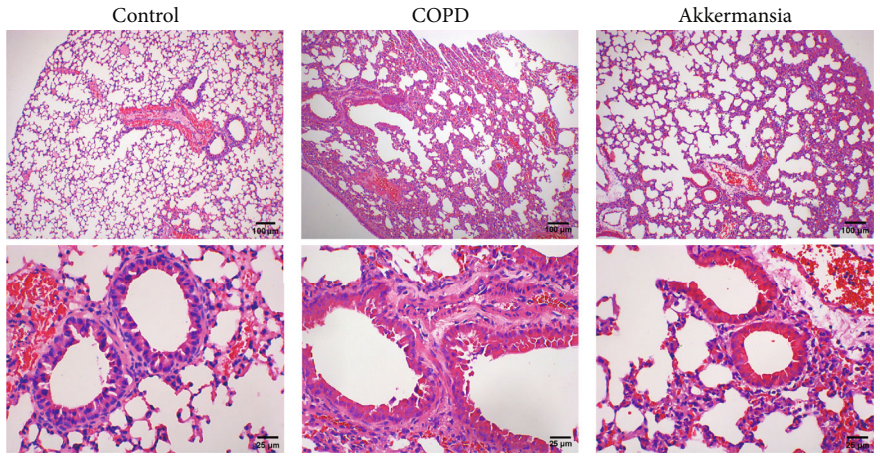

(a)

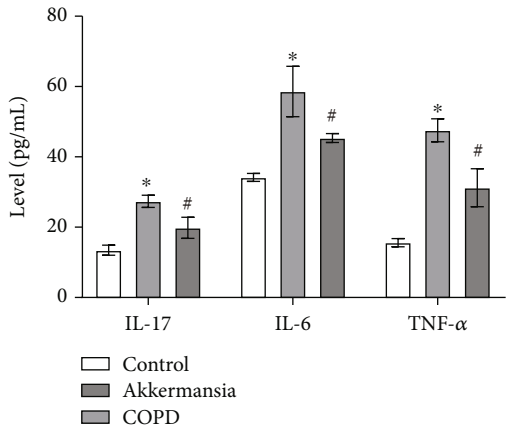

(b)

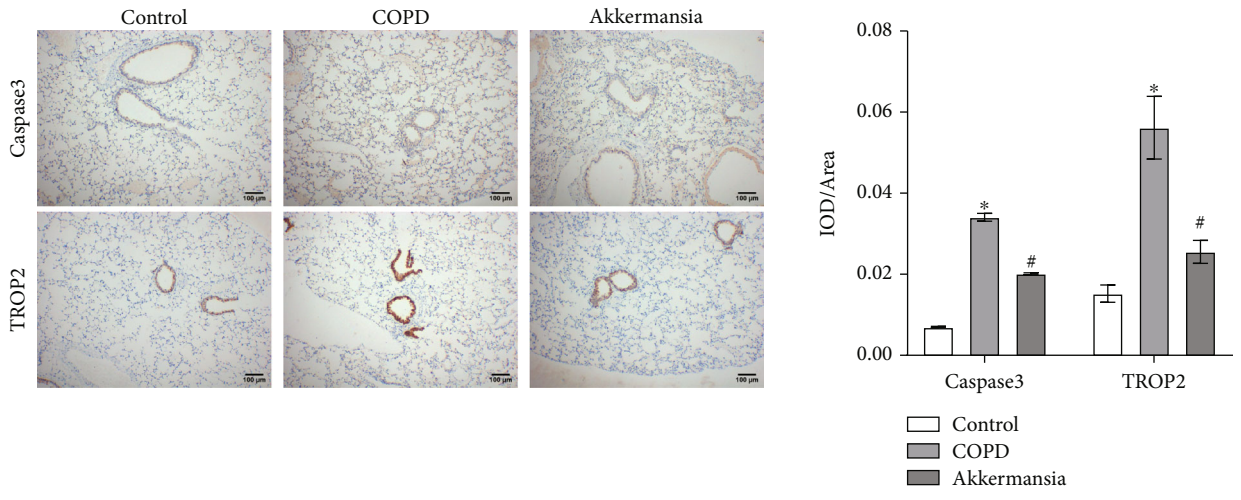

(c)

Figure 6: Continued.

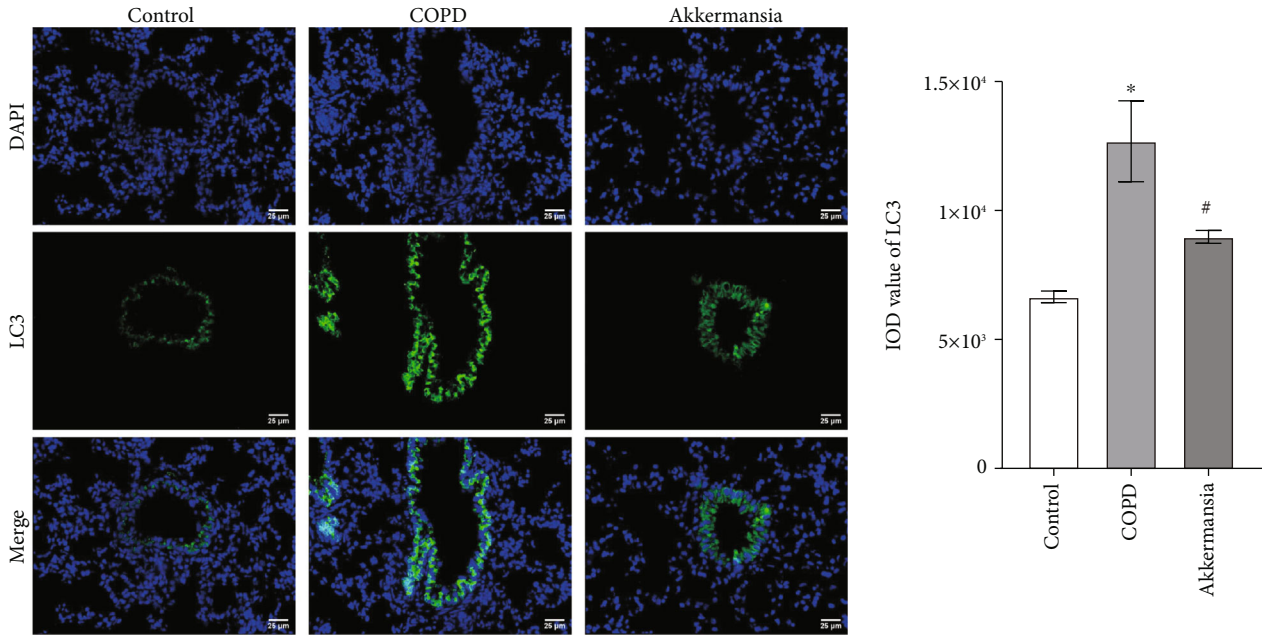

(d)

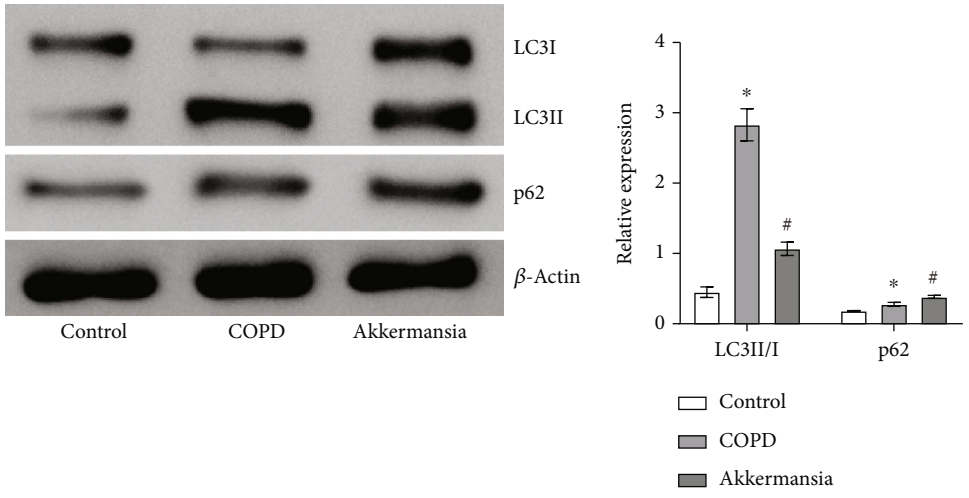

(e)

Figure 6: Continued.

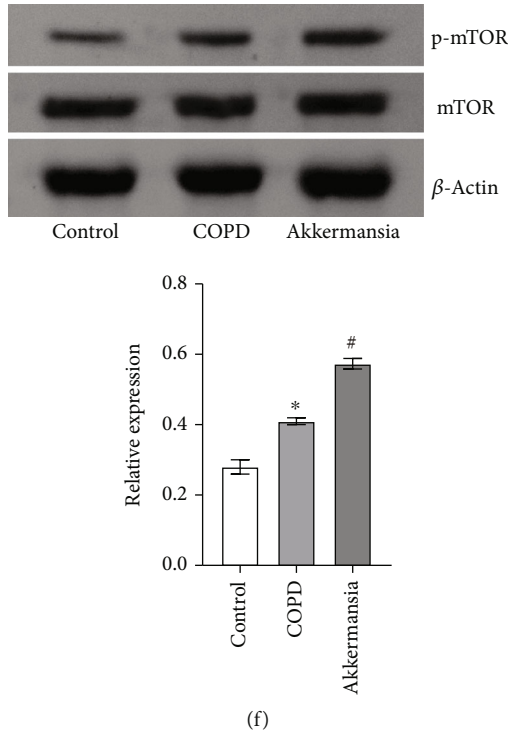

Figure 6: *Akkermansia muciniphila* improves lung tissue injury and autophagy in COPD mice. (a) HE staining was used to observe lung tissue injury. (b) The levels of IL-17A, IL-6, and TNF-α in blood were detected by ELISA. (c) The expression of cleave-caspase 3 and TROP2 was analyzed by IHC. (d) The expression of LC3 was detected by IF. (e, f) The expression of p62, LC3II/I, p-mTOR, and mTOR protein in lung tissue was analyzed via western blot. $^*P < 0.05$ vs. control; $\#P < 0.05$ vs. COPD.

could improve inflammation and autophagy induced by cigarettes in COPD mice.

4. Discussion

The immunoinflammatory processes associated with the elastin-specific T cell response are driven by cigarette smoke exposure and IL-17A [24]. The mouse model of chronic pneumonia induced by LPS/elastase demonstrated that the microbiota enhanced T cells to promote local IL-17A response, which may be a key factor leading to the development of chronic pneumonia [25]. Increased expression of IL-17A and lymphatic follicles were observed in the lung tissues of COPD patients [26]. Blocking IL17A or IL17 receptor A effectively attenuated cigarette smoke extract-induced inflammatory and MUC5AC in human bronchial epithelial cells, suggesting that IL17 mediated cigarette smoke extract-induced mucin production and inflammation in an autocrine manner [27]. Our study found that the IL-17, IL-1β, IL-6, and TNF-α levels in the peripheral blood of COPD patients were significantly increased. However, the number of intestinal microbes and alpha diversity index were decreased in COPD patients. These studies confirmed that IL-17 is a key target of smoking-induced inflammation in COPD and may be related to intestinal microbial changes.

Xuanbai Chengqi decoction corrected Th17/Treg imbalance by accumulating probiotics *Gordonia bacteria* and *Akkermansia* and greatly improved microbial homeostasis in COPD mice to reduce lung inflammation and restore lung function [28]. Low intakes of nutrients such as vitamin A, potassium, carotene, vitamin C, and retinol were significantly related to COPD [29]. Slowing proteolysis and restoring damage should be the primary goals of emphysema, with vitamin A/K, hyaluronic acid, copper, and refloats as promising candidates [30]. As a precursor of vitamin A (retinol), dietary β-carotene supplementation promotes postpartum uterine recovery by upregulating the relative abundance of *Akkermansia*, *Candidatus Stoquefichus*, and *Faecalibaculum* and inhibiting the production of inflammatory cytokines [31]. Our results showed that the abundance of *Akkermansia muciniphila* in the gut of smoking-related COPD patients might be related to retinol metabolism (retinol and retinal), which was the novelty of this work. These studies confirmed that the decrease of *Akkermansia muciniphila* in smoking-related COPD patients might be related to retinol metabolism.

Cigarette smoke extract exposure resulted in decreased Rubicon and dysregulation of LC3-associated phagocytosis in alveolar macrophages, accompanied by cytoplasmic impairment [32]. The hydroxychloroquine enhanced the increase of LC3 but not beclin1, and 3-methyladenine abolished migration and phosphorylation of p65 in cigarette smoke extract-treated cells [33]. Iofexoline played an anti-COPD role through improved lung function, anti-inflammatory, and tracheal relaxation, which was bound up with adenylyl cyclase activation, mTOR pathway, and Th17/Treg balance [34]. Probiotics maintain a balance in the gut microbiome, which leads to good health for individuals [35]. Animal experiments confirmed that *Akkermansia muciniphila*

could improve the alveolar structure and inflammatory cell infiltration in smoke-induced COPD mice, reduce the IL-17, IL-6, and TNF-α levels in peripheral blood, promote the p62 and p-mTOR expression, and inhibit the LC3 protein expression. These studies demonstrated that *Akkermansia muciniphila* could improve lung injury in smoking-induced COPD mice by mediating IL-17 and autophagy, providing new insights for the treatment of smoking-related COPD.

Retinoic acid, a metabolite of vitamin A (retinol), regulates the development of many organs and tissues and can be used as a potential therapeutic agent to improve human health [36, 37]. Milk extracellular vesicles could increase the abundance of "good" microbiota such as *Akkermansia*, *Muribaculum*, and *Turicibacter* and promote the immune related to IgA production, retinol, or D-glutamine metabolism [38]. Retinoic acid restores cholesterol levels in *Leishmania donovani*-infected macrophages and reduces the parasite burden in an mTOR-independent manner [39, 40]. Retinoic acid-liganded RARα mediates T cell activation/quiescence metabolism and differentiation of regulatory T cell subsets through PI3K and subsequent activation of Akt and mTOR signaling pathways [41]. Our study proved that the decrease of *Akkermansia muciniphila* in smoking-related COPD patients might be related to retinol metabolism. Moreover, *Akkermansia muciniphila* could improve lung injury in smoking-induced COPD mice by promoting p-mTOR expression and inhibiting IL-17 level. However, due to the constraints of research funds and time, we did not explore the underlying mechanism of retinol metabolism and mTOR signaling in *Akkermansia muciniphila*-treated COPD mice. This was a limitation in our study. Thus, further evaluation in more randomized trials and mouse experimental systems is needed.

5. Conclusion

Thus, the results of this study demonstrated that smoke induced the decrease of *Akkermansia muciniphila* abundance and alteration of retinol metabolism in COPD patients. Oral administration of *Akkermansia muciniphila* ameliorated lung injury in smoke-induced COPD mice by inflammation and autophagy, which may be the potential probiotics to treat smoke-induced COPD.

Data Availability

The data used to support the findings of this study are included within the article.

Conflicts of Interest

The authors declare that they have no conflicts of interest.

Authors' Contributions

The conceptualization was carried out by LZ and CL. Experimentation and data analysis were carried out by all authors. The experimental design was carried out by all authors. The preparation of the first draft was carried out by LZ. The manuscript revision was carried out by JL and CL. Li Zhang and Junjuan Lu are co-first authors.

Supplementary Materials

Supplementary Figure 1: KEGG function prediction of differential metabolites. *(Supplementary Materials)*

References

[1] G. E. Erhabor, B. Adeniyi, A. O. Arawomo et al., "Acute exacerbation of COPD: clinical perspectives and literature review," *West African Journal of Medicine*, vol. 38, no. 11, pp. 1129–1142, 2021.

[2] K. F. Rabe, S. Hurd, A. Anzueto et al., "Global strategy for the diagnosis, management, and prevention of chronic obstructive pulmonary disease," *American Journal of Respiratory and Critical Care Medicine*, vol. 176, no. 6, pp. 532–555, 2007.

[3] K. Sheikh, H. O. Coxson, and G. Parraga, "This is what COPD looks like," *Respirology*, vol. 21, no. 2, pp. 224–236, 2016.

[4] Y. J. Huang, J. R. Erb-Downward, R. P. Dickson, J. L. Curtis, G. B. Huffnagle, and M. K. Han, "Understanding the role of the microbiome in chronic obstructive pulmonary disease: principles, challenges, and future directions," *Translational Research*, vol. 179, pp. 71–83, 2017.

[5] Z. Wang, Y. Yang, Z. Yan et al., "Multi-omic meta-analysis identifies functional signatures of airway microbiome in chronic obstructive pulmonary disease," *The ISME Journal*, vol. 14, no. 11, pp. 2748–2765, 2020.

[6] D. Mayhew, N. Devos, C. Lambert et al., "Longitudinal profiling of the lung microbiome in the AERIS study demonstrates repeatability of bacterial and eosinophilic COPD exacerbations," *Thorax*, vol. 73, no. 5, pp. 422–430, 2018.

[7] K. L. Bowerman, S. F. Rehman, A. Vaughan et al., "Disease-associated gut microbiome and metabolome changes in patients with chronic obstructive pulmonary disease," *Nature Communications*, vol. 11, no. 1, p. 5886, 2020.

[8] H. C. Lai, T. L. Lin, T. W. Chen et al., "Gut microbiota modulates COPD pathogenesis: role of anti-inflammatory *Parabacteroides goldsteinii* lipopolysaccharide," *Gut*, vol. 71, no. 2, pp. 309–321, 2022.

[9] L. H. Cong, T. Li, H. Wang et al., "IL-17A-producing T cells exacerbate fine particulate matter-induced lung inflammation and fibrosis by inhibiting PI3K/Akt/mTOR-mediated autophagy," *Journal of Cellular and Molecular Medicine*, vol. 24, no. 15, pp. 8532–8544, 2020.

[10] R. K. Ramakrishnan, K. Bajbouj, S. Al Heialy et al., "IL-17 induced autophagy regulates mitochondrial dysfunction and fibrosis in severe asthmatic bronchial fibroblasts," *Frontiers in Immunology*, vol. 11, p. 1002, 2020.

[11] M. Reed, S. H. Morris, A. B. Owczarczyk, and N. W. Lukacs, "Deficiency of autophagy protein Map1-LC3b mediates IL-17-dependent lung pathology during respiratory viral infection via ER stress-associated IL-1," *Mucosal Immunology*, vol. 8, no. 5, pp. 1118–1130, 2015.

[12] S. P. Wiertsema, J. van Bergenhenegouwen, J. Garssen, and L. M. J. Knippels, "The interplay between the gut microbiome and the immune system in the context of infectious diseases throughout life and the role of nutrition in optimizing treatment strategies," *Nutrients*, vol. 13, no. 3, p. 886, 2021.

[13] J. Osei Sekyere, N. E. Maningi, and P. B. Fourie, "Mycobacterium tuberculosis, antimicrobials, immunity, and lung–gut microbiota crosstalk: current updates and emerging advances," *Annals of the New York Academy of Sciences*, vol. 1467, no. 1, pp. 21–47, 2020.

[14] M. Demirci, H. B. Tokman, H. K. Uysal et al., "Reduced _Akkermansia muciniphila_ and _Faecalibacterium prausnitzii_ levels in the gut microbiota of children with allergic asthma," *Allergol Immunopathol (Madr)*, vol. 47, no. 4, pp. 365–371, 2019.

[15] M. M. Pérez, L. M. S. Martins, M. S. Dias et al., "Interleukin-17/interleukin-17 receptor axis elicits intestinal neutrophil migration, restrains gut dysbiosis and lipopolysaccharide translocation in high-fat diet-induced metabolic syndrome model," *Immunology*, vol. 156, no. 4, pp. 339–355, 2019.

[16] M. Xi, J. Li, G. Hao et al., "Stachyose increases intestinal barrier through _Akkermansia muciniphila_ and reduces gut inflammation in germ-free mice after human fecal transplantation," *Food Research International*, vol. 137, article 109288, 2020.

[17] M. Thomsen, M. Dahl, P. Lange, J. Vestbo, and B. G. Nordestgaard, "Inflammatory biomarkers and comorbidities in chronic obstructive pulmonary disease," *American Journal of Respiratory and Critical Care Medicine*, vol. 186, no. 10, pp. 982–988, 2012.

[18] R. E. Walter, J. B. Wilk, M. G. Larson et al., "Systemic inflammation and COPD: the Framingham Heart Study," *Chest*, vol. 133, no. 1, pp. 19–25, 2008.

[19] A. Agustí, L. D. Edwards, S. I. Rennard et al., "Persistent systemic inflammation is associated with poor clinical outcomes in COPD: a novel phenotype," *PLoS One*, vol. 7, no. 5, article e37483, 2012.

[20] Q. Song, P. Chen, and X. M. Liu, "The role of cigarette smoke-induced pulmonary vascular endothelial cell apoptosis in COPD," *Respiratory Research*, vol. 22, no. 1, p. 39, 2021.

[21] Q. Cheng, L. Fang, D. Feng et al., "Memantine ameliorates pulmonary inflammation in a mice model of COPD induced by cigarette smoke combined with LPS," *Biomedicine & Pharmacotherapy*, vol. 109, pp. 2005–2013, 2019.

[22] Q. Liu, H. Li, Q. Wang et al., "Increased expression of TROP2 in airway basal cells potentially contributes to airway remodeling in chronic obstructive pulmonary disease," *Respiratory Research*, vol. 17, no. 1, p. 159, 2016.

[23] K. A. Stringer, M. Tobias, H. C. O'Neill, and C. C. Franklin, "Cigarette smoke extract-induced suppression of caspase-3-like activity impairs human neutrophil phagocytosis," *American Journal of Physiology. Lung Cellular and Molecular Physiology*, vol. 292, no. 6, pp. L1572–L1579, 2007.

[24] J. S. Zhou, Z. Y. Li, X. C. Xu et al., "Cigarette smoke-initiated autoimmunity facilitates sensitisation to elastin-induced COPD-like pathologies in mice," *The European Respiratory Journal*, vol. 56, no. 3, article 2000404, 2020.

[25] K. Yadava, C. Pattaroni, A. K. Sichelstiel et al., "Microbiota promotes chronic pulmonary inflammation by enhancing IL-17A and autoantibodies," *American Journal of Respiratory and Critical Care Medicine*, vol. 193, no. 9, pp. 975–987, 2016.

[26] J. Xiong, L. Zhou, J. Tian et al., "Cigarette smoke-induced lymphoid neogenesis in COPD involves IL-17/RANKL pathway," *Frontiers in Immunology*, vol. 11, article 588522, 2020.

[27] M. Wu, T. Lai, D. Jing et al., "Epithelium-derived IL17A promotes cigarette smoke-induced inflammation and mucus hyperproduction," *American Journal of Respiratory Cell and Molecular Biology*, vol. 65, no. 6, pp. 581–592, 2021.

[28] Y. Wang, N. Li, Q. Li et al., "Xuanbai Chengqi decoction ameliorates pulmonary inflammation via reshaping gut microbiota and rectifying Th17/Treg imbalance in a murine model of chronic obstructive pulmonary disease," *International Journal of Chronic Obstructive Pulmonary Disease*, vol. Volume 16, pp. 3317–3335, 2021.

[29] H. J. Park, M. K. Byun, H. J. Kim et al., "Dietary vitamin C intake protects against COPD: the Korea National Health and Nutrition Examination Survey in 2012," *International Journal of Chronic Obstructive Pulmonary Disease*, vol. Volume 11, pp. 2721–2728, 2016.

[30] R. Janssen, I. Piscaer, F. M. E. Franssen, and E. F. M. Wouters, "Emphysema: looking beyond alpha-1 antitrypsin deficiency," *Expert Review of Respiratory Medicine*, vol. 13, no. 4, pp. 381–397, 2019.

[31] X. Yang, Z. He, R. Hu et al., "Dietary β-carotene on postpartum uterine recovery in mice: crosstalk between gut microbiota and inflammation," *Frontiers in Immunology*, vol. 12, article 744425, 2021.

[32] P. F. Asare, H. B. Tran, P. R. Hurtado et al., "Inhibition of LC3-associated phagocytosis in COPD and in response to cigarette smoke," *Therapeutic Advances in Respiratory Disease*, vol. 15, 2021.

[33] Y. Le, Y. Wang, L. Zhou et al., "Cigarette smoke-induced HMGB1 translocation and release contribute to migration and NF-κB activation through inducing autophagy in lung macrophages," *Journal of Cellular and Molecular Medicine*, vol. 24, no. 2, pp. 1319–1331, 2020.

[34] C. Xiao, S. Cheng, H. Lin et al., "Isoforskolin, an adenylyl cyclase activator, attenuates cigarette smoke- induced COPD in rats," *Phytomedicine*, vol. 91, article 153701, 2021.

[35] G. U. Varela-Trinidad, C. Domínguez-Díaz, K. Solórzano-Castanedo, L. Íñiguez-Gutiérrez, T. J. Hernández-Flores, and M. Fafutis-Morris, "Probiotics: protecting our health from the gut," *Microorganisms*, vol. 10, no. 7, p. 1428, 2022.

[36] J. L. Napoli, "Retinoic acid: the autacoid for all seasons," *Nutrients*, vol. 14, no. 21, p. 4526, 2022.

[37] N. B. Ghyselinck and G. Duester, "Retinoic acid signaling pathways," *Development*, vol. 146, no. 13, p. 13, 2019.

[38] C. Du, S. Quan, X. Nan et al., "Effects of oral milk extracellular vesicles on the gut microbiome and serum metabolome in mice," *Food & Function*, vol. 12, no. 21, pp. 10938–10949, 2021.

[39] S. Prakash and A. K. Rai, "Retinoic acid increases cellular cholesterol in Leishmania donovani-infected macrophages in an mTOR-independent manner," *Microbiol Spectr.*, vol. 10, no. 6, article e0269922, 2022.

[40] S. Prakash and R. A. Kumar, "Retinoic acid increases the cellular cholesterol predominantly in a mTOR-independent manner," *Immunologic Research*, vol. 70, no. 4, pp. 530–536, 2022.

[41] L. R. Friesen, B. Gu, and C. H. Kim, "A ligand-independent fast function of RARα promotes exit from metabolic quiescence upon T cell activation and controls T cell differentiation," *Mucosal Immunology*, vol. 14, no. 1, pp. 100–112, 2021.